Original Article

Micro-Computed Tomographic Evaluation of Fetal Skeletal Changes Induced by All-*Trans*-Retinoic Acid in Rats and Rabbits

L. David Wise,* Dahai Xue, and Christopher T. Winkelmann

Merck Research Laboratories, West Point, Pennsylvania

BACKGROUND: Our laboratory has been conducting positive control studies to evaluate the utility of micro-computed tomography (micro-CT) for qualitative evaluation of fetal skeletal morphology. All-*trans*-retinoic acid (atRA) was used to produce a different spectrum of defects compared to our previous studies with boric acid and hydroxyurea. **METHODS:** Groups of five mated Crl:CD(SD) female rats each were administered vehicle or atRA (2.5–50 mg/kg) on GD 10, and groups of four mated Dutch Belted rabbits each were dosed with vehicle or atRA (6.25–25 mg/kg) on GD 9. Cesarean sections were performed on GD 21 and 28, respectively. Following external examination the viscera were removed and fetuses scanned in a micro-CT imaging system. Fetuses were subsequently stained with alizarin red. Skeletal morphology was evaluated by each method without the knowledge of treatment group. Total bone mineral content (BMC) of each fetus was quantitated using the micro-CT images. **RESULTS:** In rats there were dose-related increases in the incidence of extra lumbar vertebra and non-dose-related increases in supernumerary ribs at all dose levels. There were decreases in mean number of ossified sacrocaudal vertebra at $\geq$5 mg/kg, and increases in skull bone malformations at $\geq$10 mg/kg. Rabbits were less sensitive on a mg/kg basis since skeletal malformations and a decrease in mean number of ossified sacrocaudal vertebra were observed only in the 25-mg/kg group. Micro-CT evaluation detected essentially the same incidence of skeletal abnormalities as seen in alizarin red-stained rat and rabbit fetuses. BMC analysis showed a trend toward slight decreases in atRA-treated rats, but no notable changes in rabbits. **CONCLUSIONS:** These results add support to our previous work that demonstrates that micro-CT imaging can effectively assess rat and rabbit fetal skeletal morphology. *Birth Defects Res (Part B)* 89:408–417, 2010. © 2010 Wiley-Liss, Inc.

Key words: ***all-trans-retinoic acid; retinoic acid; skeletal evaluation; micro-Computed Tomography; micro-CT; developmental toxicity; alizarin red staining***

INTRODUCTION

Merck Research Laboratories have been exploring the use of micro-computed tomography (micro-CT) for the evaluation of fetal skeletal morphology as part of safety assessment studies such as the embryo-fetal developmental (EFD) toxicity studies in rats and rabbits. Utilizing the capabilities of the GE eXplore Locus Ultra micro-CT, up to ~400 rat fetuses or ~200 rabbit fetuses can be scanned ex vivo per hour at an isotropic spatial resolution of 185 μm (Winkelmann and Wise, 2009). This level of throughput is more than adequate for inclusion in EFD studies since a total of 80 litters are usually scheduled for routine cesarean section over 2 to 4 consecutive days. Previous positive control studies in rats with boric acid (Wise and Winkelmann, 2009a) and in rabbits with hydroxyurea (Wise and Winkelmann, 2009b) have assessed the utility of the technology with particular attention to assessing whether or not the resolution of this micro-CT system is adequate for the identification of various induced skeletal abnormalities. In these previous studies there was a high concordance of findings observed between micro-CT and alizarin red staining; both methods revealed the same major skeletal malformation and variations in rat and rabbit fetuses. The specific findings that did not exactly match involved the very smallest skeletal elements and/or those elements with a minimal degree of ossification. These previous positive control studies produced defects predominately of the axial skeleton although some skull defects were observed in rabbits at the highest dose level. In order to gain additional experience with micro-CT evaluations of other skeletal regions we conducted the present positive control studies with all-*trans*-retinoic acid (atRA), which is known to produce various skull

*Correspondence to: L. David Wise, Merck Research Laboratories, Safety Assessment, WP 45-115, West Point, PA 19486.
E-mail: ld_wise@merck.com
Received 15 June 2010; Accepted 26 July 2010
Published online in Wiley Online Library (wileyonlinelibrary.com).
DOI: 10.1002/bdrb.20267

Table 1
Rat Cesarean Section and Fetal Skeletal Examinations

	All-trans-retinoic acid (mg/kg) on GD 10													
	Control 1*		Control 2**		2.5**		5**		10**		25*		50*	
Fetuses/litters evaluated	60/5		64/5		64/5		63/5		57/5		64/5		66/5	
Female fetal weight (g)	5.25		5.32		5.53		5.17		5.05		5.07		4.91	
Percent below control							3%		5%		3%		6%	
Male fetal weight (g)	5.43		5.67		5.88		5.27		5.54		5.42		5.21	
Percent below control							7%		2%		–		4%	
% Postimplantation loss	3.3%		1.5%		3.2%		1.7%		7.5%		3.1%		1.3%	
	Stain	mCT	Stain	mCT	Stain	mCT	Stain	mCT	Stain	mCT	Stain	mCT	Stain	mCT
Torso and Limbs														
Fetuses with Malformation	0	0	1	4	**5**	**4**	**29**	**27**	**48**	**47**	**62**	**62**	**66**	**66**
% Litter Mean	0%	0%	1.7%	6.3%	**7.5%**	**5.9%**	**48%**	**45%**	**84%**	**83%**	**97%**	**97%**	**100%**	**100%**
Fetuses with Variation	9	6	3	3	**29**	**24**	**29**	**28**	**35**	**27**	**24**	**19**	**20**	**13**
% Litter Mean	14%	9%	5%	5%	**45%**	**37%**	**48%**	**47%**	**62%**	**45%**	**38%**	**30%**	**30%**	**20%**
Fetuses with Inc. Oss.	2	2	6	3	4	0	3	8	**10**	**13**	**23**	**25**	**45**	**50**
% Litter Mean	3.5%	3.5%	9.3%	4.3%	5.7%	0%	5.2%	12%	**18%**	**30%**	**37%**	**40%**	**68%**	**76%**
Head														
Fetuses with Malformation	0	0	0	0	0	1	1	3	**8**	**9**	**58**	**58**	**66**	**66**
% Litter Mean	0%	0%	0%	0%	0%	1.4%	1.4%	5.1%	**21%**	**24%**	**91%**	**91%**	**100%**	**100%**
Fetuses with Variation	0	0	0	0	0	1	0	0	0	0	0	0	0	0
% Litter Mean	0%	0%	0%	0%	0%	1.5%	0%	0%	0%	0%	0%	0%	0%	0%
Fetuses with Inc. Oss.	2	2	2	13	3	5	5	11	0	5	**23**	**25**	**45**	**50**
% Litter Mean	3.5%	3.5%	3.3%	22%	5.4%	8.9%	7.6%	18%	0%	15%	**37%**	**40%**	**68%**	**76%**
Skeletal Findings														
Absent skull bone (M)	0	0	0	0	0	1	0	1	0	0	1	**7**	**24**	**30**
Small skull bone (M)	0	0	0	0	0	1	0	2	0	0	**27**	**22**	**6**	**8**
Skull bone malf.	0	0	0	0	0	0	1	1	**5**	**3**	**53**	**51**	**59**	**59**
Skull bone fusion (M)	0	0	0	0	0	0	0	0	0	0	**23**	**34**	**55**	**59**
Tympanic annulus malf.	0	0	0	0	0	0	1	1	**8**	**8**	**3**	**5**	**28**	**36**
Supern.skull bone (M)	0	0	0	0	0	0	0	0	1	0	0	0	1	1
Extra vertebra (M)	0	0	0	0	**4**	**3**	**29**	**27**	**48**	**47**	**62**	**62**	**65**	**65**
Thoracic vertebra malf.	0	0	0	0	1	1	0	0	0	0	**4**	**3**	**6**	**5**
Lumbar vertebra malf.	0	0	0	0	0	0	0	0	0	0	**3**	**3**	**14**	**16**
Axial skeleton malf.	0	0	0	0	0	0	1	1	0	0	1	1	**20**	**19**
Cervical vertebra malf.	0	0	0	1	0	0	0	0	0	0	0	0	0	0
Sacral vertebra malf.	0	0	0	0	0	0	0	0	0	0	2	2	0	0
Fused ribs (M)	0	0	0	0	0	0	0	0	0	0	0	0	**8**	**8**
Absent rib (M)	1	1	1	1	0	0	0	0	0	0	0	1	2	3
Discontinuous rib (M)	0	0	0	0	0	0	0	0	0	0	0	0	1	0
Hypoplastic rib (M)	0	0	0	2	0	0	0	1	0	1	1	0	0	1
Detached rib (M)	0	0	0	0	0	0	0	0	1	0	0	0	1	0
Sternebral malf.	0	0	0	0	0	0	0	0	1	0	0	0	0	0
Skull bone variation	0	0	0	0	0	1	0	0	0	0	0	0	0	0
Lumbar vertebra variation	0	0	0	0	0	0	0	0	1	0	0	0	1	2

Table 1
Continued

	All-trans-retinoic acid (mg/kg) on GD 10													
	Stain	mCT	Stain	mCT	Stain	mCT	Stain	mCT	Stain	mCT	Stain	mCT	Stain	mCT
Cervical rib variation	1	1	0		0	0	0	0	0	0	0	0	0	0
Supernumerary rib (V)	8	5	3		3	**29**	**24**	**29**	**28**	**33**	**27**	**24**	**19**	**10**
Wavy rib (V)	0	0	1		0	0	0	0	0	0	0	0	0	0
Sternebral variation	0	0	0		0	0	0	0	0	2	0	0	0	0
Pelvic bone variation	0	0	0		0	0	1	0	1	0	0	0	0	1
Inc. Oss. skull bone	0	0	0		1	0	0	0	1	0	0	0	0	1
Inc. Oss. cervical vertebra	0	0	0		0	0	0	0	2	0	0	1	0	0
Inc. Oss. thoracic vertebra	0	0	6		3	4	0	2	2	**10**	**11**	**15**	**36**	**37**
Inc. Oss. lumbar vertebra	0	0	0		0	0	0	0	0	2	3	**18**	**22**	**24**
Inc. Oss. sternebra	2	2	0		0	0	0	1	4	1	5	0	0	5
Inc. Oss. hyoid	0	1	2		12	3	5	5	10	0	5	1	1	1
Mean ossified SCV	11.4	10.2	10.4		9.5	10.6	9.4	**10.1**	**9.0**	**9.5**	**8.6**	**10.5**	**10.5**	**9.4**
Percent below control								**3%**	**5%**	**9%**	**9%**	**8%**	**8%**	**8%**

*Study 1.
**Study 2.
M and malf, malformation; V, variation; Inc. Oss., incomplete ossification; SCV, sacrocaudal vertebrae.
Bold and underlined finding are considered to be test article-related.

defects in rats (Martinez-Angoa et al., 2006). In this study micro-CT evaluations again effectively identified all skeletal abnormalities.

MATERIALS AND METHODS

Animal Husbandry

The studies were conducted at Merck Research Laboratories (West Point, PA). Mated female Sprague–Dawley [Crl:CD(SD)] rats were obtained from Charles River Laboratories (Raleigh, NC). Mated female Dutch Belted rabbits were obtained from Covance Research Products (Denver, PA). Female rats and rabbits were approximately 10 and 25 weeks of age, respectively, on Gestation Day (GD) 0 (the day of confirmed mating with males of the same strain). All animals were identified by a microchip implant and delivered to the laboratory on GD 1 or 7. Animal housing and care procedures were in compliance with the Federal Animal Welfare Act and the Institute for Laboratory Animal Resources. All procedures performed on the animals were reviewed and approved by an Institutional Animal Care and Use Committee. The animal facility is fully accredited by the Association for Assessment and Accreditation of Laboratory Animal Care International.

Presumed pregnant female rats and rabbits were individually housed in suspended, stainless-steel, wire-bottom cages in environmentally controlled rooms with an approximate 12-hr light/dark cycle. All rats had free access to PMI certified rodent diet and water throughout the study. Beginning on the day of arrival, rabbits received 100 g/day of PMI certified rabbit diet and small amounts of fresh fruit and/or vegetables. All rabbits also had free access to water throughout the study.

Animals were observed daily for mortality and physical signs with an additional observation made 1 to 5 hr postdosing. All females were weighed frequently during gestation.

Test Agent

atRA (99% pure) was obtained from Sigma-Aldrich, Inc. (St. Louis, MO). Solutions at designated concentrations were prepared in corn oil (also from Sigma-Aldrich, Inc.) in order to deliver a dose volume of 5 ml/kg for rats and 1 ml/kg for rabbits.

Experimental Design and Procedures

Two separate rat studies and one rabbit study were performed. The rat studies utilized groups of five mated females each. The first rat study administered 0 (vehicle only), 25, or 50 mg/kg of atRA once on GD 10 by oral gavage. Since this first study found a very high incidence of skeletal malformations, a second rat study conducted approximately 6 months later administered 0, 2.5, 5, or 10 mg/kg also by oral gavage on GD 10. This day of treatment matches that of other investigators (Tembe et al., 1996; Johnson et al., 2008). The rabbit study utilized groups of four mated females each and dose levels of 0, 6.25, 12.5, and 25 mg/kg administered once by oral gavage on GD 9. Rabbits were treated one day earlier since embryonic development on GD 9 appeared to be most similar to that of GD 10 rat embryos (DeSesso, 2006).

Rats were euthanized on GD 21 by CO_2 asphyxiation, and rabbits on GD 28 by an intravenous injection of sodium pentobarbital. Females were given a blind-code number so that fetuses would be examined without the knowledge of treatment group. The location and number of implantations were recorded and each classified as live fetus, dead fetus, or resorption. All fetuses were weighed, sexed (rat only), and examined externally for abnormalities. Fetuses were euthanized by oral administration of sodium pentobarbital, and then thoracic and abdominal viscera were removed.

Methods for micro-CT scanning have been described previously (Winkelmann and Wise, 2009). In brief, each litter was placed into a custom-made polystyrene holder that contained labels to identify the blind-code number of the dam/doe and the number of each fetus. Each holder was positioned in the micro-CT gantry for image acquisition. Micro-CT images were acquired using the GE eXplore Locus Ultra (GE Healthcare, United Kingdom) with X-ray settings of 80 kV and 50 mA using the 16 sec anatomical protocol, which collects 1000 projections in a single 360° gantry rotation. The projection data for each scan was reconstructed using the AxRecon reconstruction system (Acceleware, Calgary, Canada). The reconstructed image slices consisted of 100 μm isotropic voxels scaled to Hounsfield units (HU). Spatial resolution of the micro-CT system is hardware limited and is reported by the manufacturer to be 185 μm. The reconstructed slices of the entire scan were then processed using a custom program to segment each fetus and save the fetus image data into individual image files. Individual fetal images were then manually evaluated for skeletal abnormalities using the software visualization program Amira 5.1 (Visage Imaging, Andover, MA) and applying VolrenGlow colormaps in the Voltex module. After scanning, all fetuses were fixed and stained with alizarin red by standard methods (Redfern and Wise, 2007) for subsequent skeletal examination. Both fetal images and stained specimens were evaluated without the knowledge of treatment group by a small group of experienced evaluators. Inter-observer variation was not assessed.

Quantitative bone mineral content (BMC) data for each fetal skeleton were also obtained as follows. Each fetal image was segmented by using a threshold of 180 HU. Voxels with values of 180 HU and above were considered bone and included in the segmentation. The threshold value was chosen by visual examination of the fetal images at several different threshold values; 180 HU was chosen because it did not include soft tissue (lower thresholds) and did not exclude small and/or thin skeletal structures, such as distal phalanges or thin skull bones (higher thresholds). The segmented voxels (at 180 HU and above) were then passed through a size filter to remove any structures smaller than 20 continuous voxels. These small structures were considered high-frequency noise associated with the images. The remaining voxels were counted to obtain total fetal bone volume, and the included "bone" voxel values were averaged to obtain an average bone intensity value in HU. This average HU intensity value was then converted to bone mineral density (BMD) with units of mg/cc of hydroxyapatite by use of a custom density calibration phantom (Mindways, Inc., Austin, TX). The HU values of the individual density rods of the phantom were measured separately in the micro-CT images using Amira, and a linear regression curve was generated according to the phantom manufacturer's instructions to give a calibration curve converting HU to mg/cc of hydroxyapatite. This calibration curve was then used to convert average HU bone intensity values to average BMD of the entire skeleton of each fetus. BMC for each fetus was then obtained by simple multiplication of BMD and bone volume. Fetal BMC values were averaged to obtain a litter mean BMC. Litter mean BMC values were then averaged by dose group to obtain group mean BMC and standard deviation.

Data Analysis

Determination of atRA-related effects used a variety of nonstatistical tools, which consisted of absolute or relative reference to the concurrent control, comparisons to an extensive historic control database, evaluation of the inherent variability of a given parameter, and evaluation of dose–response relationships. Based on these evaluations, a judgment was made that categorized a change as test article-related or not.

RESULTS

F_0 Females

No unscheduled deaths occurred during the studies, and the few observed physical signs were of the type seen in vehicle-treated rats and rabbits in this laboratory and were considered unrelated to treatment. There were no effects on F_0 female body weights during gestation (data not shown).

Cesarean Sections

In rats there were no effects of atRA on embryonic and fetal survival as shown by percent postimplantation loss (Table 1). There were slight decreases in mean live fetal weights in the groups administered $\geq$5 mg/kg (2–7% below control, Table 1); however, the decreases were not dose-related and therefore of questionable relationship to treatment with atRA. The fetal incidence of atRA-related external malformations in the 50-mg/kg group was 80% and involved primarily the eye (exophthalmia), ears (anotia, microtia, detached, or malpositioned pinna), and cleft palates (data not shown). In the 10- and 25-mg/kg groups, the incidence of similar external malformations was very low (i.e., 6 and 2 affected fetuses, respectively).

In rabbits there were no effects of atRA treatment on percent postimplantation loss or mean live fetal weights (Table 2). External malformations were observed only in the 25-mg/kg group and consisted of small ears (43%) and absent or small tails (75%).

Fetal Skeletal Evaluations

In rats the most prevalent skeletal malformation was a dose-related increased incidence of extra lumbar vertebra in all atRA-treated groups. The incidences were almost exactly the same by the two evaluation methods (Table 1) with differences of only 1 or 2 fetuses in two groups (Table 1). atRA also induced various skull bone malformations in rat fetuses at dose levels $\geq$10 mg/kg, and again micro-CT identification was comparable to the alizarin red evaluation. The following elements were

Table 2
Rabbit Cesarean Section and Fetal Skeletal Examinations

	All-*trans* retinoic acid (mg/kg) on GD 9							
	Control		6.25		12.5		25	
Fetuses/litters evaluated	23/4		20/4		23/4		23/4	
Fetal weight (g)	35.1		33.2		33.8		34.1	
% Postimplantation loss	7.7%		28.1%		0%		15.5%	
	Stain	mCT	Stain	mCT	Stain	mCT	Stain	mCT
Torso and Limbs								
Fetuses with Malformation	0	0	0	0	0	0	**16**	**16**
% Litter Mean	0%	0%	0%	0%	0%	0%	**69%**	**69%**
Fetuses with Variation	0	0	2	2	7	7	1	0
% Litter Mean	0%	0%	7.1%	7.1%	31%	31%	4.2%	0%
Fetuses with Inc. Oss.	3	5	0	1	2	2	1	1
% Litter Mean	13%	22%	0%	3.6%	9.5%	8.9%	4.2%	6.3%
Head								
Fetuses with Malformation	1	0	0	0	0	0	**2**	**2**
% Litter Mean	4.2%	0%	0%	0%	0%	0%	**13%**	**13%**
Fetuses with Variation	0	0	0	0	0	0	0	0
Fetuses with Inc. Oss.	1	0	0	0	1	0	2	4
% Litter Mean	4.2%	0%	0%	0%	4.2%	0%	10%	21%
Skeletal Findings								
Skull bone M	0	0	0	0	0	0	**2**	**2**
Craniostenosis (M)	1	0	0	0	0	0	0	0
Lumbar vertebra M	0	0	0	0	0	0	1	1
Sacral vertebra M	0	0	0	0	0	0	2	1
Axial skeleton M	0	0	0	0	0	0	**4**	**4**
Caudal vertebra M	0	0	0	0	0	0	**9**	**10**
Hypoplastic rib (M)	0	0	0	0	0	0	0	1
Short 13th rib (V)	0	0	2	2	7	7	1	0
Inc. Oss. cervical vertebra	2	0	0	0	2	1	0	0
Inc. Oss. caudal vertebra	0	0	0	0	0	0	1	0
Inc. Oss. sternebra	1	2	0	0	0	0	0	1
Inc. Oss. metacarpal	0	3	0	1	0	1	0	0
Inc. Oss. hyoid	1	0	0	0	1	0	2	4
Mean ossified SCV	19.5	18.9	19.7	18.8	19.6	19.1	**12.8**	**12.5**
% below control							**34%**	**34%**

M, malformation; V, variation; Inc. Oss., incomplete ossification; SCV, sacrocaudal vertebrae.
Bold and underlined finding are considered to be test article-related.

most often absent, small, or misshapen (Fig. 1): squamosal, zygomatic, tympanic annulus, and pterygoid processes. Skull bone fusions most often involved the premaxilla to the maxilla, zygomatic to zygomatic process of maxilla (Fig. 2), and/or the pterygoid processes of the basisphenoid to the palatine bones.

The most prevalent skeletal variation in rat fetuses was a non-dose-related increased incidence of supernumerary 14th (i.e., ''lumbar'') rib(s) in all atRA-treated groups (Table 1) that was observed by both methods of evaluation. This variation was present in nearly all fetuses with extra lumbar vertebra in the 2.5- and 5-mg/kg groups, but at $\geq$10 mg/kg there were more fetuses with extra lumbar vertebra (Fig. 3). The incidence of supernumerary rib was slightly lower by micro-CT evaluation in most groups since, as reported previously (Wise and Winkelmann, 2009a), the very smallest extra ribs (i.e., trace ossification sites) are not observed due to the spatial resolution limitation of micro-CT. However, despite this limitation, micro-CT clearly identified that all dose levels were affected. The remaining axial skeletal abnormalities (i.e., thoracic and lumbar vertebra malformation, axial skeletal malformation [malformations of vertebrae in 2 or more regions], incomplete ossification of the thoracic and/or lumbar vertebra, and fused ribs) showed excellent agreement between the two methods of evaluation (i.e., not more than two fetuses different between the two methods). In rats the mean numbers of ossified sacrocaudal vertebrae identified by micro-CT were slightly less in all groups compared to the alizarin red evaluation, which was also due to the spatial resolution limitation of micro-CT. However, relative to the concurrent control, there were comparable decreases in the mean numbers of ossified sacrocaudal vertebrae by both evaluation methods at dose levels $\geq$5 mg/kg.

In rabbits, the skeletal abnormalities were observed only in the 25-mg/kg group, and that incidence of affected fetuses was lower than the same dose level in rats (69 vs. 97%, respectively). The skeletal malformations involved mainly the vertebrae, although two fetuses had skull bone malformations (Table 2 and Figs. 4 and 5). The predominant skeletal malformations of the skull, axial skeleton, and caudal vertebra were correctly identified by micro-CT evaluation. There were no skeletal

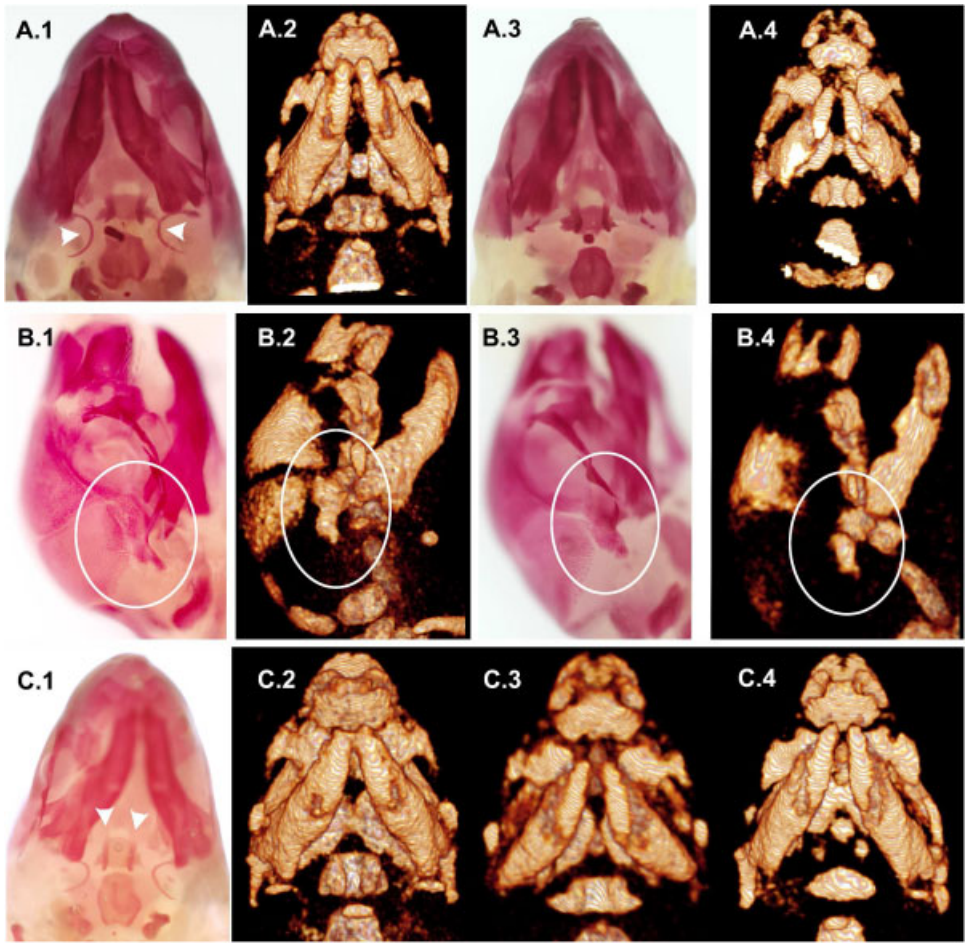

Fig. 1. Alizarin red stained (white background) and micro-CT images (black background) of rat fetuses. **A.1** and **A.2**: ventral view of skull showing normal tympanic annulus (arrowheads). **A.3** and **A.4**: atRA-exposed fetuses with absent tympanic annulus. **B.1** and **B.2**: right-side lateral view of skull showing normal squamosal bone (center of oval). **B.3** and **B.4**: atRA-exposed fetuses with misshapen squamosal bone. **C.1** and **C.2**: ventral view of skull showing normal pterygoid processes protruding from the basisphenoid bone. **C.3** and **C.4**: misshapen and absent pterygoid processes.

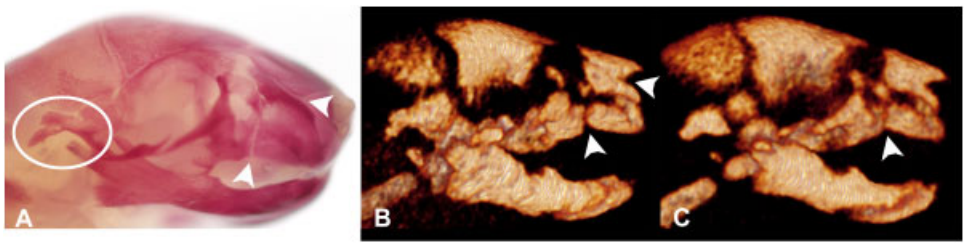

Fig. 2. Right lateral view of normal rat skull stained with alizarin red (**A**) and micro-CT image (**B**) showing normal squamosal bone (oval) and maxilla-premaxilla and premaxilla-nasal sutures (arrowheads). Abnormal fetus (**C**) showing misshapen squamosal, abnormal zygomatics, and fusion of maxilla to premaxilla (arrowhead) and probably fusion of premaxilla to nasal bone.

malformations in the 6.25- and 12.5-mg/kg groups. There was a notable decrease in the mean number of ossified sacrocaudal vertebrae in the 25-mg/kg group by both evaluation methods (both 34% below control, Table 2), which was related to the tail malformations.

Fetal BMC

We investigated obtaining unique quantitative data from the micro-CT images by measuring BMC for each fetus. Figure 6 shows results for mean BMC in rats and rabbits. There were trends toward slight decreases in mean BMC at the higher dose levels in rats compared to the concurrent control groups. There were no meaningful changes in mean BMC in the rabbit study. The BMC of rabbits is approximately 10-fold greater than rats at these ages (GD 28 and GD 21, respectively). However, when fetal weight is taken into account, BMC per gram of body weight for rabbits is approximately 2-fold greater than rats. This relative increase in BMC could be

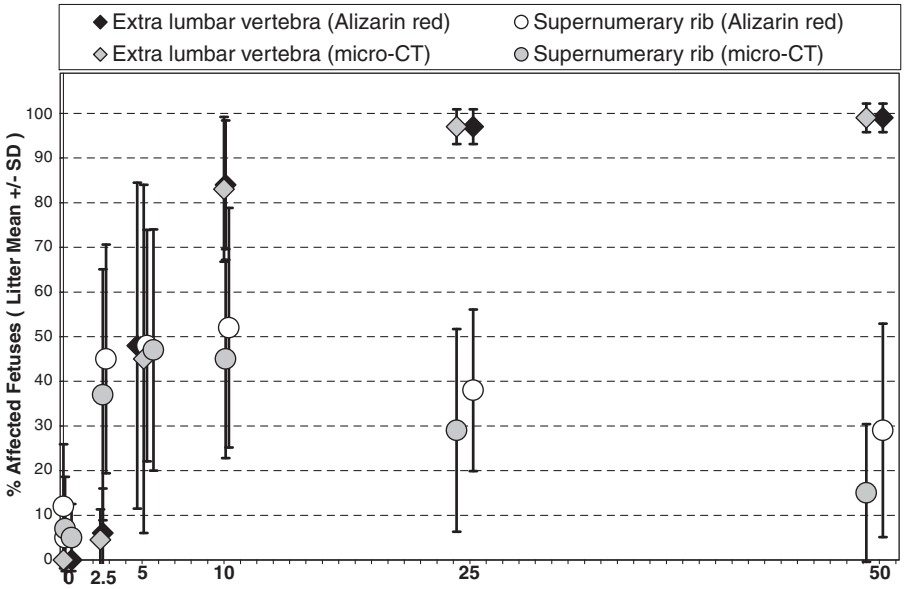

Fig. 3. Litter mean incidences of extra lumbar vertetra and supernumerary rib in rat fetuses exposed to various dose levels of all-*trans*-retinoic acid (atRA). There was a dose-related increase in litter mean incidence of extra lumbar vertetra, and a non-dose-related increase in the incidence of supernumerary rib that appeared to peak in the 10-mg/kg group. Note the very close concordance of both findings by alizarin red stain and micro-CT evaluations.

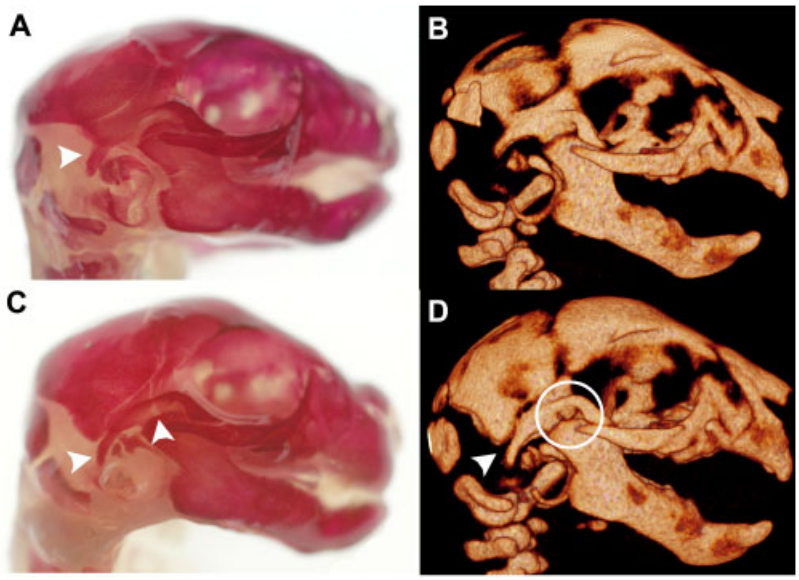

Fig. 4. Alizarin red stained and micro-CT images of rabbit fetuses showing right lateral view of normal skull (**A** and **B**); arrowhead points to post tympanic process of squamosal. **C** and **D**: fetus with misshapen squamosal bone at arrowheads and oval.

attributed to greater skeletal development due to the increased gestational age of the rabbits. It is noteworthy that the two vehicle control rat groups showed differences in mean BMC (Study 1 is 17% below Study 2). There was also a slight difference in mean fetal body weight between these two vehicle control groups (control male fetuses in Study 1 were 4% below Study 2), which is not unexpected given different shipments of rats. Figure 5 also shows the relatively high correlation between individual fetal rat and rabbit body weights and BMC.

DISCUSSION

The utility of micro-CT in the evaluation of skeletal development is beginning to be recognized (Guldberg et al., 2004; Johnson et al., 2006; Oest et al., 2008). Our laboratory has been examining the use of this imaging technology for qualitative evaluations of skeletal morphology as required for EFD toxicity studies. Along with the present work, our collective studies show that micro-CT is comparable to traditional alizarin red skeletal evaluations (Wise and Winkelmann, 2009a,b). In addition,

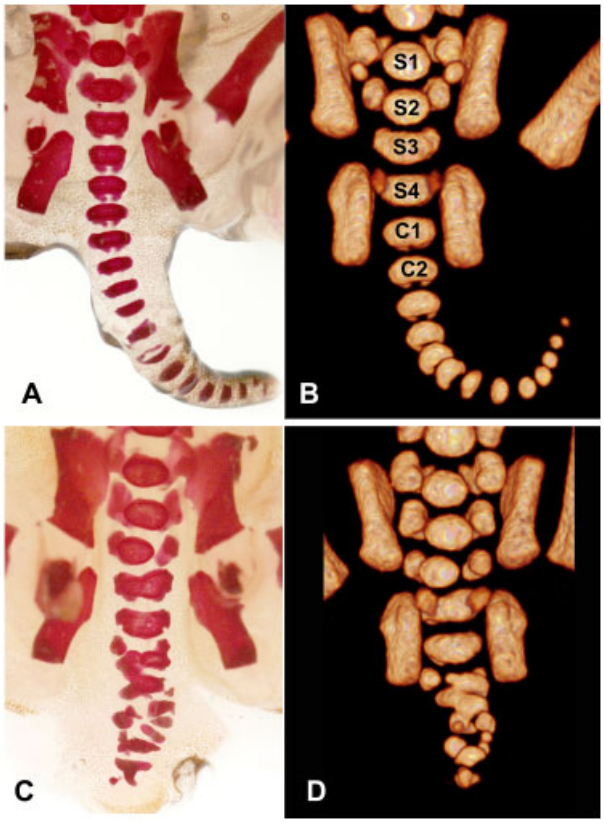

Fig. 5. Alizarin red stained and micro-CT images of rabbit fetuses showing ventral view of normal sacral and caudal area (**A** and **B**) and fetus with misshapen sacral and caudal vertebrae, which is termed axial skeletal malformation (**C** and **D**, see Table 2).

due to the capabilities of the micro-CT system in our laboratory we have demonstrated that all litters from a typical EFD study (i.e., ~20 litters per day across four consecutive days) can be easily scanned (Winkelmann and Wise, 2009).

It is readily apparent that different micro-CT systems have different resolutions. The system utilized in our studies to-date is able to scan one litter in only 16 sec, and produces images with a spatial resolution of 185 μm. As discussed previously (Wise and Winkelmann, 2009a), this resolution does not allow visualization of distinct skeletal elements that are less than approximately 0.3 mm in diameter or adjacent to each other. Other systems produce images of higher resolution (e.g., 100 μm or less), but require significantly longer scan times. In addition, those other systems usually do not allow the simultaneous scan of one complete litter as can be performed with the system in our laboratory.

To our knowledge the utility and necessity of higher resolution has not been addressed. Our data support the claim that 185-μm resolution of micro-CT images is adequate for qualitative evaluation of rat and rabbit fetal skeletons. This resolution does not always allow visualization of the very smallest skeletal elements, which includes the following: phalanges, caudal-most vertebrae, distal sternebral centers, the hyoid, and trace supernumerary ribs (either cervical or lumbar). Because of their variable degree of ossification some, if not many, laboratories only evaluate these small skeletal elements as either present or absent, or may merely count the number of alizarin red-stained ossified elements in a given region. As pointed out by Carney and Kimmel (2007), minor delays in ossification seem to be readily repairable via postnatal remodeling, and would not generally be considered adverse in and of themselves. Supernumerary rib has received the most attention (Chernoff and Rogers, 2004). Trace extra lumbar ossification sites in rat fetuses are not readily detected by micro-CT; however, these "rudimentary lumbar ribs" are transient by most accounts and are not toxicologically meaningful. Both cervical ribs and "extra" lumbar ribs (i.e., greater than half the length of the 13th rib) are potentially signals of developmental toxicity. We have shown with boric acid that micro-CT at 185-μm resolution was readily able to detect cervical ribs (Wise and Winkelmann, 2009a), and the present study with atRA demonstrates that increases in the incidence of supernumerary ribs was readily observed with the resolution of our micro-CT system. It is most likely that other micro-CT systems with higher resolution will allow a somewhat more accurate evaluation of such small ossification sites; however, the cost for doing so will be lower throughput due to slower scan times. This discussion of optimal resolution and throughput will no doubt diminish as this technology advances.

Our past and present positive control studies have obviously not encountered all possible skeletal abnormalities. If the recent publication by Makris et al. (2009) is taken as the complete listing, then there are 1019 possible skeletal abnormalities (including those of cartilage). Based on our experience to-date, and with the caveats noted above, we are confident that the vast majority of skeletal malformations and variations of bone will be detected with micro-CT. What is perhaps most important to risk assessment is the identification of potentially hazardous dose levels of a new compound. Such determinations require an evaluation of all available data from the study in question, and often from other studies conducted in-house or from the literature. It is well recognized that a developmental toxicant will most often affect a number of developing organs/bones when administered during the period of major organogenesis. Indeed, this has been seen in our past and present positive control studies. More precisely, although certain skeletal abnormalities in individual fetuses may be "missed" or accentuated by micro-CT evaluation, the studies clearly demonstrate that correct identification of developmental toxicity at a group level is readily apparent.

An interesting finding from the present study was the dose-related increase in extra lumbar vertebra together with the non-dose-related increase in supernumerary ribs in rats (Fig. 3). The mechanism for these findings is unknown. There are at least two general, perhaps overlapping explanations. Assuming the embryonic compartment contains a mixture of teratogenic atRA-related compounds (i.e., parent and metabolites) after dosing, then the induction of each of the two abnormalities may involve different compounds. Alternatively, or in addition, both abnormalities may be induced by the same teratogenic compound(s) but the molecular developmental pathways are sufficiently different in specifics and/or timing such that extra lumbar vertebra shows a

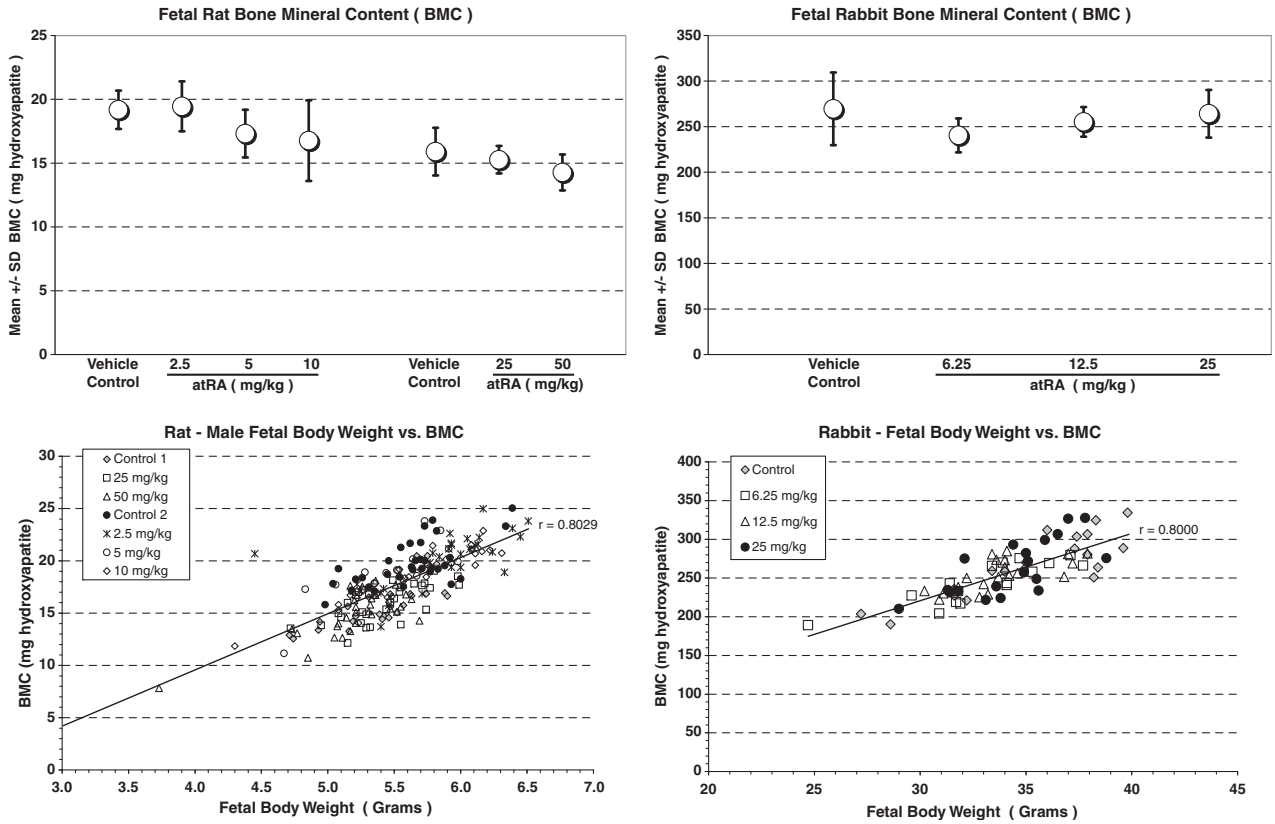

Fig. 6. Upper panels: Litter mean (±SD) bone mineral content (BMC) in rat and rabbit fetuses. Lower panels: scatter plots of individual rat and rabbit fetal body weights and BMC. There is a relatively good correlation between these parameters ($r \geq 0.8$).

dose-related response and supernumerary rib shows a non-dose-related response. Clearly, further work is required for an explanation to this phenomenon.

Fetal rabbits appeared to be less sensitive to atRA-induced defects on a mg/kg basis compared to rat fetuses under the single-dose conditions of these studies. The decreased sensitivity to atRA is consistent with Tembe et al. (1996) who reported that oral dose levels of 10, 20, or 30 mg/kg given on GD 10 to NZW rabbits did not produce a significant incidence of either external malformations or resorptions compared to corn oil dosed controls, whereas Wistar rats showed multiple defects with 20 and 30 mg/kg given on GD 10.

Although the analysis of BMC of rat fetuses showed only slight decreases at the higher dose levels compared to the concurrent controls and no suggestion of an atRA-effect in rabbit fetuses, we anticipate that BMC analysis will be potentially useful in future studies. Such analyses will be able to detect a generalized test article-related effect on bone mineralization that may or may not be associated with a generalized effect on fetal body weight. In addition, BMC analysis can be readily automated to provide results quickly with little to no manpower expenditure.

Given the close concordance of skeletal findings observed in our present and past studies, the implementation of micro-CT evaluation has many advantages over conventional alizarin red staining. As previously stated by us and others, these advantages may be summarized as follows. Micro-CT decreases the time to begin skeletal evaluations, the resources associated with hazardous staining solutions, the risks of staining artifacts, and the resources required to archive wet fetal specimens (vs. electronic images). Micro-CT increases the ability to retrieve and share images, and reclaims laboratory space used for staining and evaluations. In addition, micro-CT will facilitate a variety of new and different means to assess potential developmental toxicity. Some examples that are under investigation in this laboratory include longitudinal studies of postnatal skeletal maturation, quantitative measurements (e.g., bone lengths, volumes, and BMC), and automatic segmentation of skeletal elements for subsequent automatic or semi-automatic evaluations. Despite the substantial cost to purchase, install, and operate a micro-CT scanner, the instrument would certainly have multiple applications within a large laboratory or institution. Finally, with the aid of contrast agents, micro-CT will also allow investigators to perform evaluations of visceral morphology on the same fetuses (Johnson et al., 2006; Metscher, 2009). This imaging technology clearly holds great promise as the next generation methodology for skeletal assessment, especially in high-throughput studies conducted in the chemical and pharmaceutical industries.

ACKNOWLEDGMENTS

We gratefully acknowledge the expert technical skills provided by many personnel within the Departments of Safety Assessment and Imaging, Merck Research Laboratories.

REFERENCES

Carney EW, Kimmel CA. 2007. Interpretation of skeletal variations for human risk assessment: Delayed ossification and wavy ribs. Birth Defects Res B Dev Reprod Toxicol 80:473–496.

Chernoff N, Rogers JM. 2004. Supernumerary ribs in developmental toxicity bioassays and in human populations: incidence and biological significance. J Toxicol Environ Health B 7:437–449.

DeSesso JM. 2006. Comparative features of vertebrate embryology. In: Hood RD, editor. Handbook of developmental toxicology. New York: CRL Press, Inc. p 147–197.

Guldberg RE, Lin ASP, Coleman R, et al. 2004. Microcomputed tomography imaging of skeletal development and growth. Birth Defects Res C Embryo Today 72:250–259.

Johnson JT, Hansen MS, Wu I, et al. 2006. Virtual histology of transgenic mouse embryos for high-throughput phenotyping. PLoS Genet 2: 471–477.

Johnson K, Davis J, Ryan L, Moser G. 2008. Application of micro-computed tomography in rat teratology studies. Birth Defects Res A Clin Mol Teratol 82:311.

Makris SL, Solomon HM, Clark R, et al. 2009. Terminology of developmental abnormalities in common laboratory mammals (Version 2). Birth Defects Res B Dev Reprod Toxicol 86:227–327.

Martinez-Angoa A, Parra-Hernandez E, Madrigal-Bujaidar E, et al. 2006. Reduction of all-trans-retinoic acid-induced teratogenesis in the rat by glycine administration. Birth Defects Res A Clin Mol Teratol 76:731–738.

Metscher BD. 2009. MicroCT for developmental biology: a versatile tool for high-contrast 3D imaging at histological resolutions. Dev Dynam 238:632–640.

Oest M, Jones JC, Hatfield C, Prater MR. 2008. Micro-CT evaluation of murine fetal skeletal development yields greater morphometric precision over traditional clear-staining methods. Birth Defects Res B Dev Reprod Toxicol 83:582–589.

Redfern BG, Wise LD. 2007. High-throughput staining for the evaluation of fetal skeletal development in rats and rabbits. Birth Defects Res B Dev Reprod Toxicol 80:177–182.

Tembe EA, Honeywell R, Buss NE, Renwick AG. 1996. All-trans-retinoic acid in maternal plasma and teratogenicity in rats and rabbits. Tox Appl Pharm 141:456–472.

Winkelmann CT, Wise LD. 2009. High-throughput micro-computed tomography imaging as a method to evaluate rat and rabbit fetal skeletal abnormalities for developmental toxicity studies. J Pharm Tox Methods 59:156–165.

Wise LD, Winkelmann CT. 2009a. Micro-computed tomography and alizarin red evaluations of boric acid-induced fetal skeletal changes in Sprague-Dawley rats. Birth Defects Res B Dev Reprod Toxicol 86: 214–219.

Wise LD, Winkelmann CT. 2009b. Evaluation of hydroxyurea-induced fetal skeletal changes in Dutch Belted rabbits by micro-computed tomography and alizarin red staining. Birth Defects Res B Dev Reprod Toxicol 86:220–226.